Supplementary Materials

Stable performance of supported PdO_x catalyst on mesoporous silica-alumina of water tolerance for methane combustion under wet conditions

Minseok Kim [1,†], Suhyun Lim [1,†], Chansong Kim [2], Chae-Ho Shin [2], Joon Hyun Baik [3], and Young-Woong Suh [1,4,*]

[1] Department of Chemical Engineering, Hanyang University, Seoul 04763, Republic of Korea

[2] Department of Chemical Engineering, Chungbuk National University, Cheongju 28644, Republic of Korea

[3] Department of Chemical and Biological Engineering, Sookmyung Women's University, Seoul 04310, South Korea

[4] Research Institute of Industrial Science, Hanyang University, Seoul 04763 Republic of Korea

Number of Pages: 10, Number of Figures: 8, Number of Tables: 1

*Corresponding author. E-mail: ywsuh@hanyang.ac.kr; Phone: +82-2-2220-2329; ORCID: 0000-0002-2094-0724 (Y.-W. Suh)

[†]The authors contributed equally to this work.

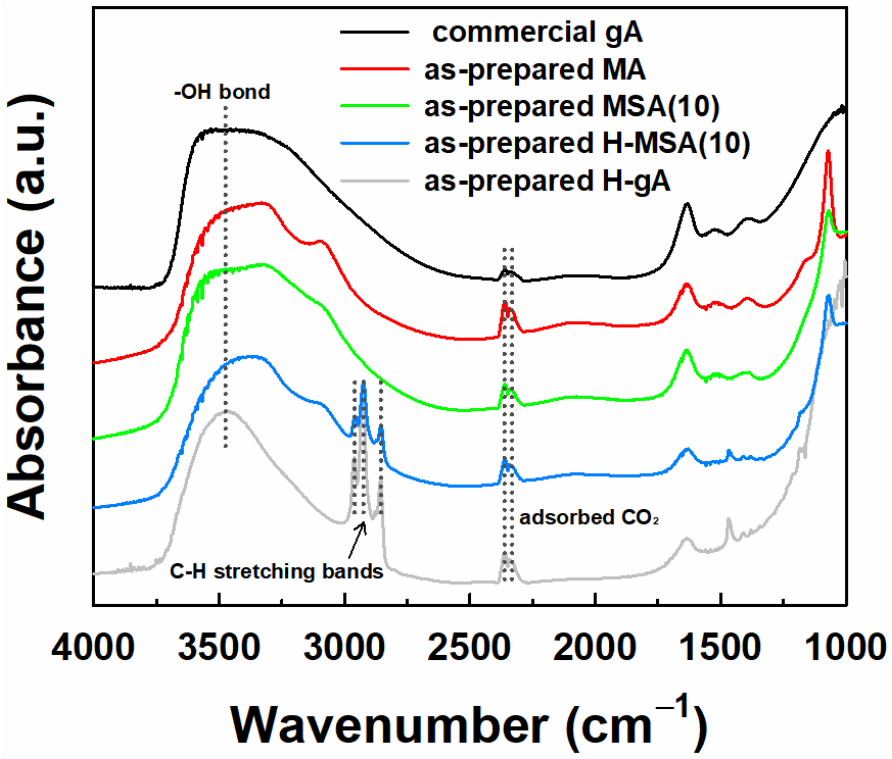

Figure S1. FT-IR spectra of the as-synthesized samples (H-MSA(10), MSA(10), MA and gA) and water-tolerant γ-alumina (H-gA).

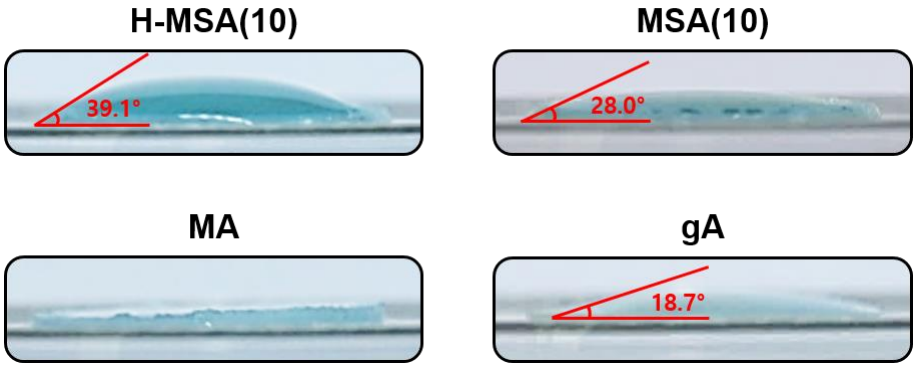

Figure S2. Wettability experiments with H-MSA(10), MSA(10), MA, and gA. The measured contact angle is added into each panel except MA showing the spreading behavior.

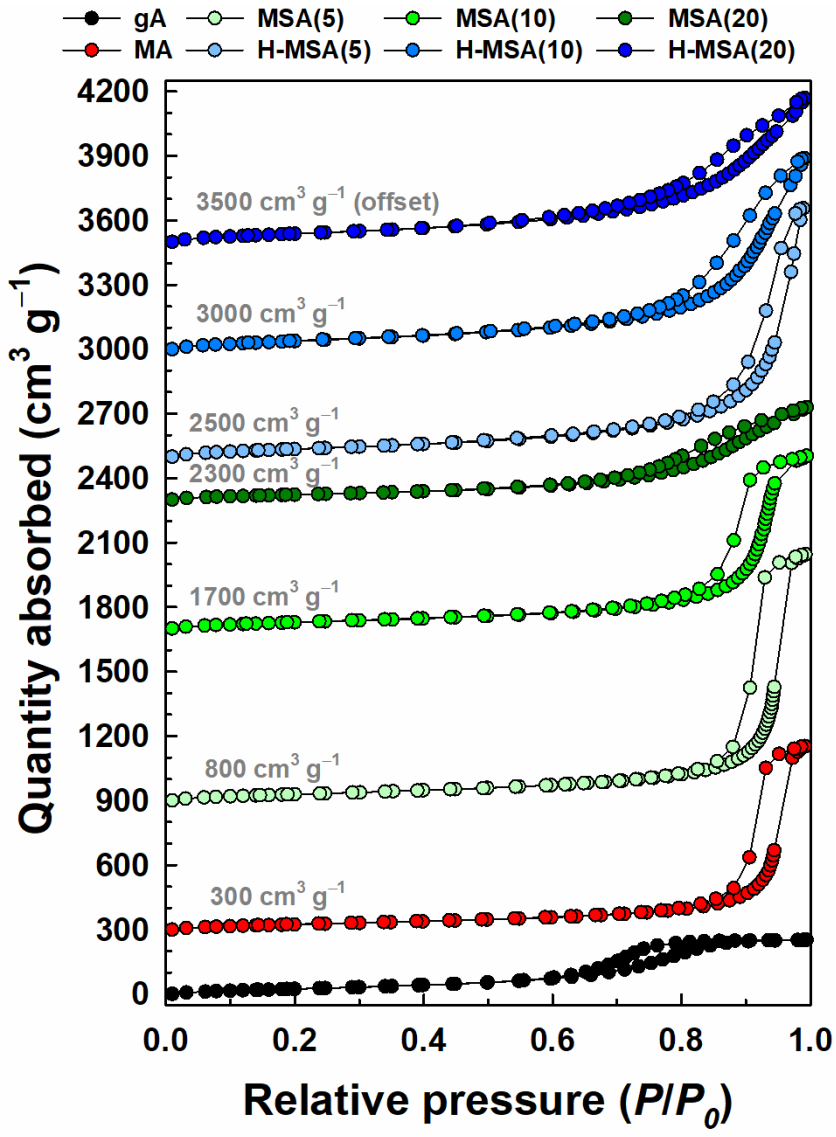

Figure S3. N_2 adsorption-desorption isotherms of the prepared support materials.

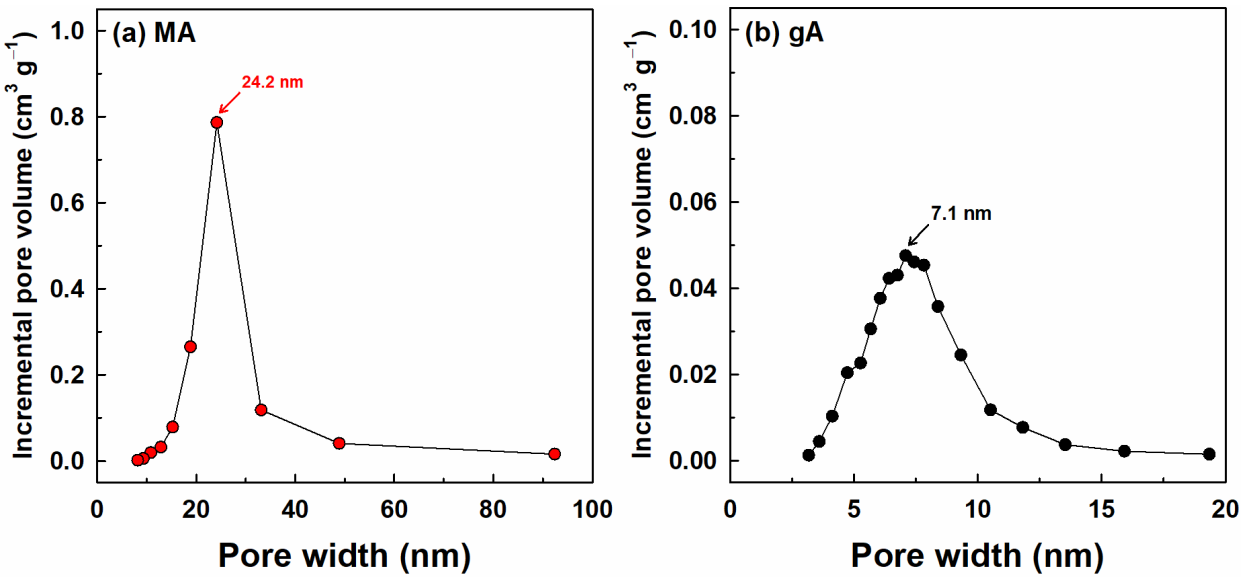

Figure S4. Pore size distribution curves of the prepared support materials: (a) MA and (b) gA.

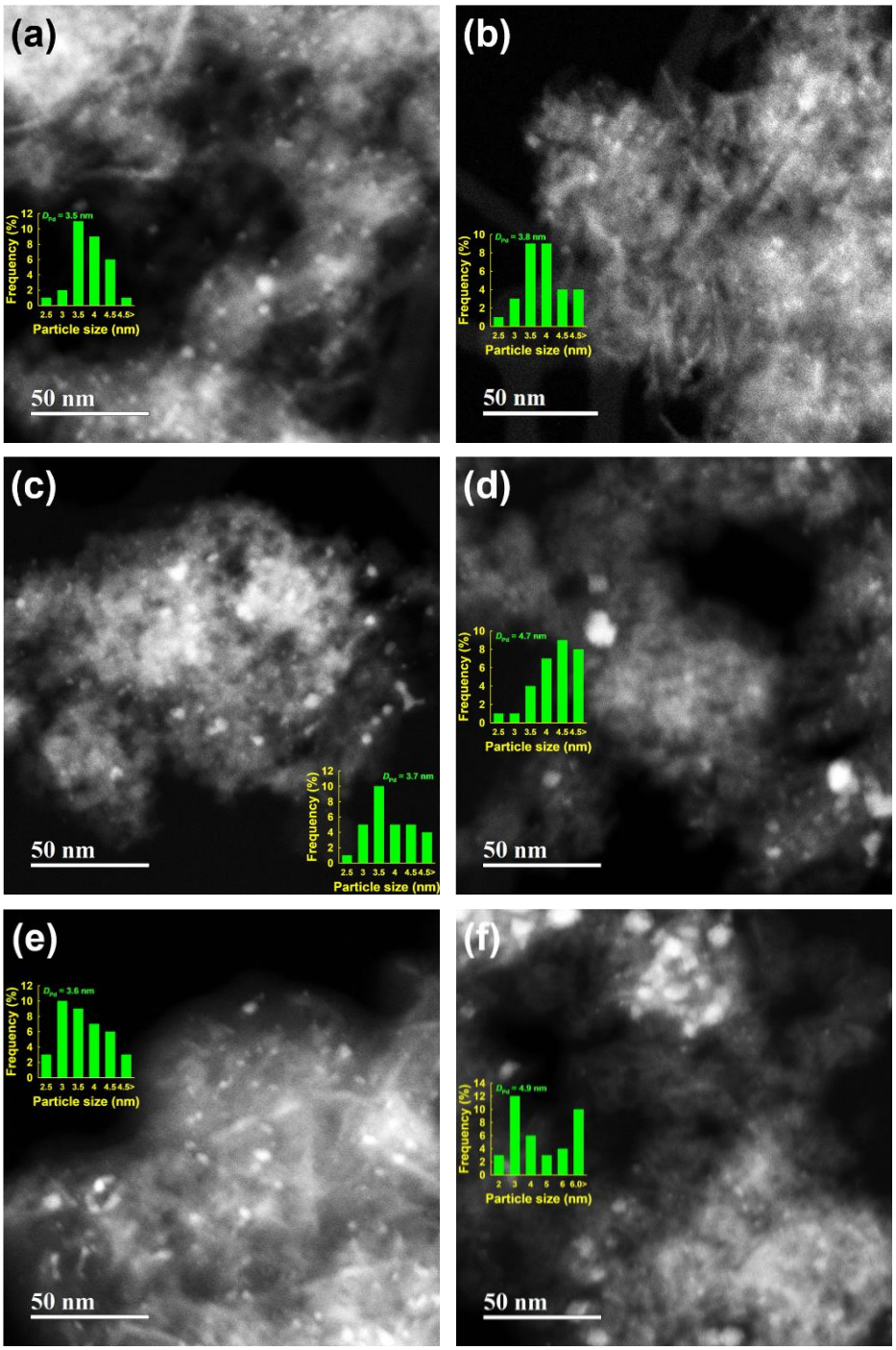

Figure S5. TEM images of (a) the fresh PdO_x/H-MSA(10), (b) spent PdO_x/H-MSA(10), (c) fresh PdO_x/MSA(10), (d) spent PdO_x/MSA(10), (e) fresh PdO_x/MA, and (f) spent PdO_x/MA. The spent samples were obtained after isothermal test at 500 °C for 24 h. Insets represent the particle size distribution of PdO_x determined by statistical analysis of ca. 30–40 white particles.

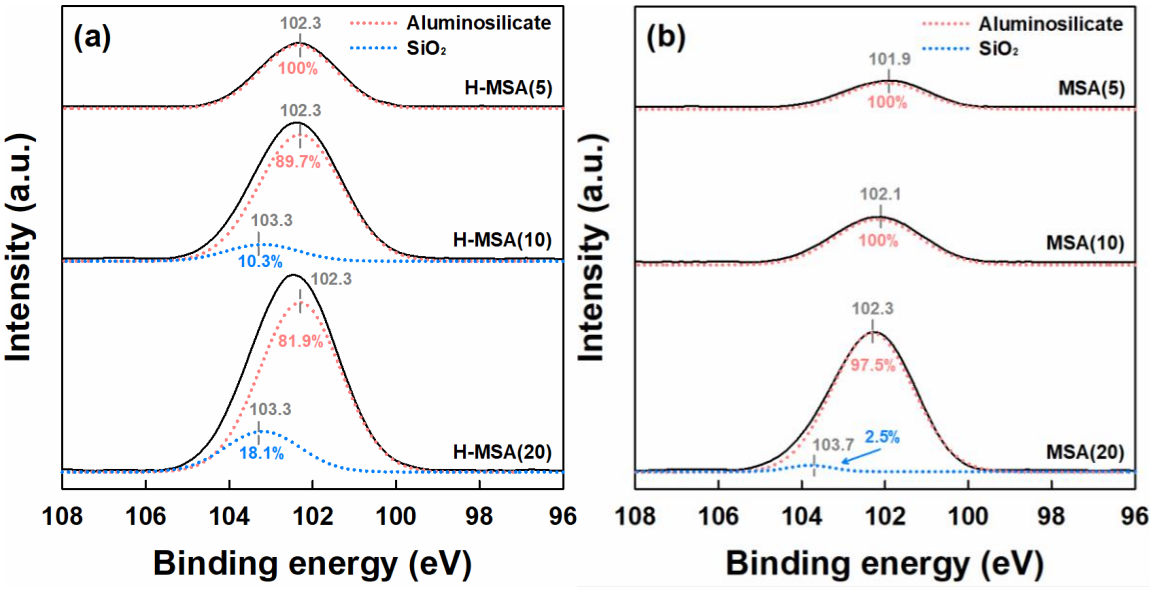

Figure S6. XPS results of (a) H-MSA(*x*) and (b) MSA(*x*) in the binding energy region of Si 2p.

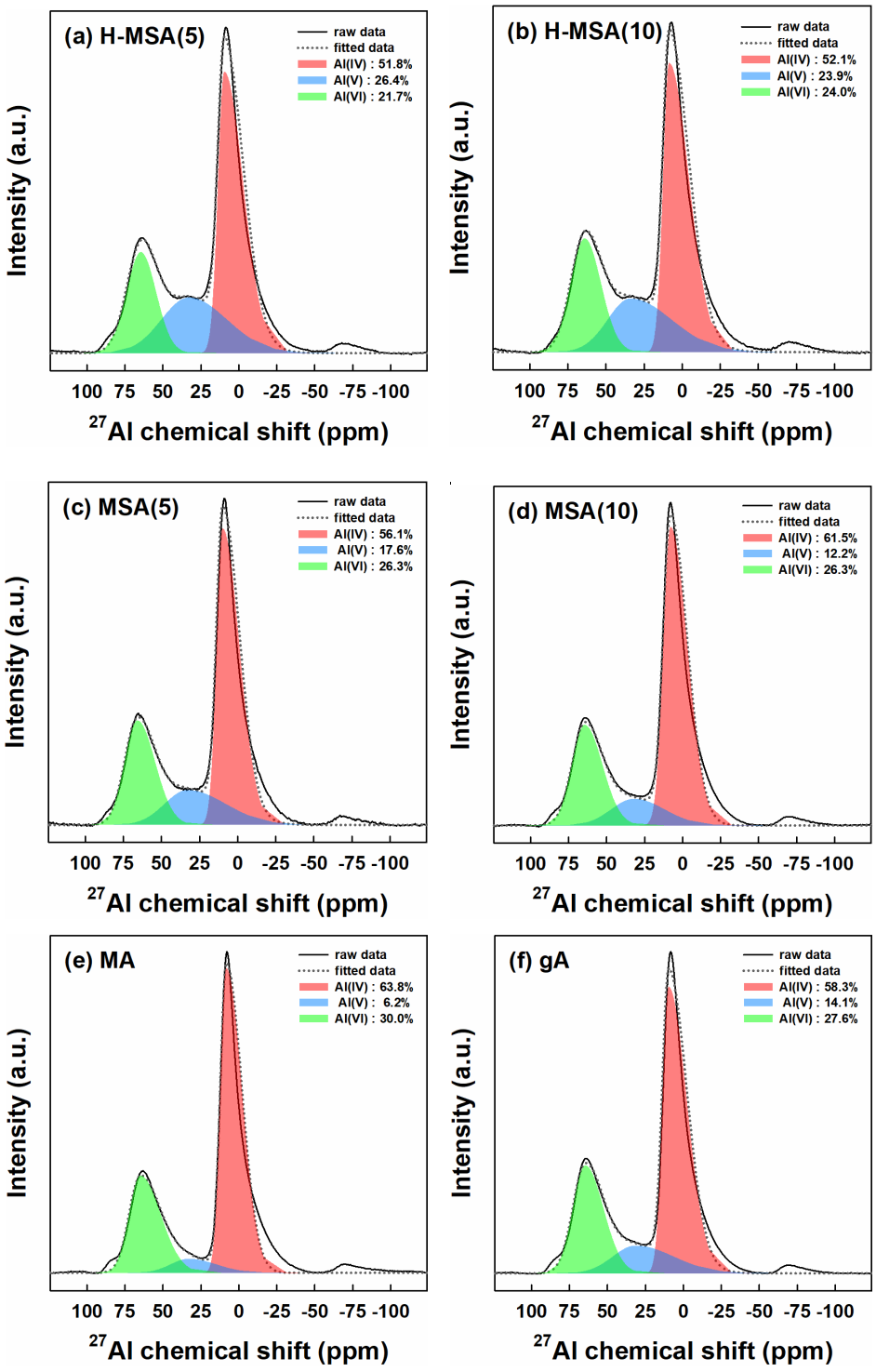

Figure S7. ^{27}Al MAS NMR spectra of all supports: (a) H-MSA(5), (b) H-MSA(10), (c) MSA(5), (d) MSA(10), (e) MA and (f) gA (red: octahedral Al^{VI}; blue: penta-coordinated Al^{V}; green: tetrahedral Al^{IV}). The fitting results are marked by gray dots.

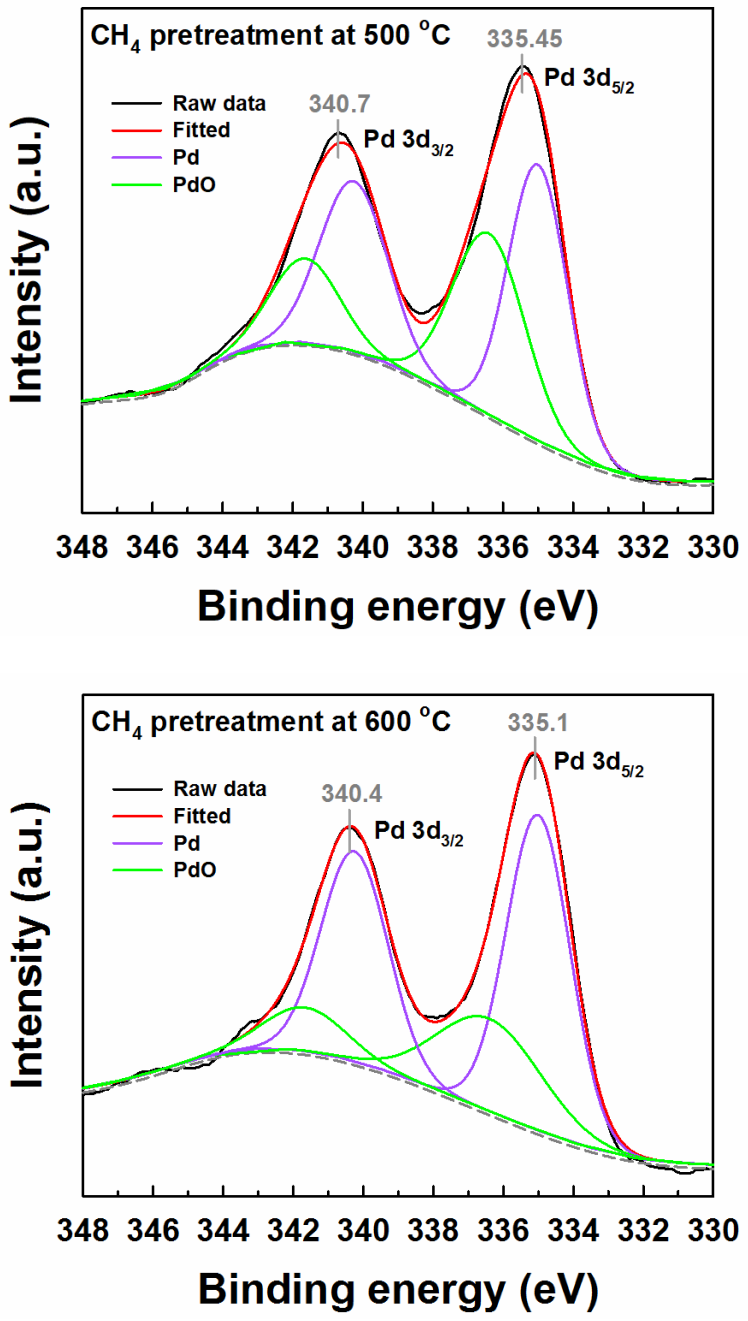

Figure S8. XPS spectra of the catalyst samples pretreated with 20% CH_4 in N_2 at 500 and 600 °C.

Table S1. Isothermal methane combustion performance of the reported Pd catalysts and PdO_x/H-MSA(5) in this work

Catalyst	Feed composition				GHSV	Temp.	CH_4 conv.	Ref.
	CH_4 (%)	O_2 (%)	H_2O (%)	Balance gas	($cm^3\ g^{-1}\ h^{-1}$)	(°C)	(%)	
Pd/κ-CZ	1	20	5	N_2	30,000	330	60	[1]
Pd2Ce	0.07	8.5	10	N_2	36,000	425	65	[2]
Al-Pd/MA-A72	0.5	10	10	N_2	40,000	500	95	[3]
0.6Pd@S-1	1	16	4.5	N_2	50,000	410	95	[4]
Pd/5CZA-5M	1	5	5	N_2	50,000	360	50	[5]
Pd/Na-MOR-Dno	1	4	5	N_2	70,000	410	92	[6]
1.1Pd-SSZ-13(16)	0.15	5	10	He	100,000	400	99	[7]
Pd/TS-1	0.7	-	3–4	air	100,000	400	92	[8]
PdCe	0.5	2	10	He	180,000	450	55	[9]
PdCe SCS	0.5	2	10	He	200,000	450	50	[10]
Pd/ZrO_2(85)	0.1	3.15	10	N_2	240,000	500	95	[11]
Pd/ZrO_2(700)	0.1	3.15	10	N_2	240,000	450	97.5	[12]
PdO_x/H-MSA(5)	0.4	12	5	N_2	200,000	500	98	This work

References

1. Ding, Y.; Wu, Q.; Lin, B.; Guo, Y.; Guo, Y.; Wang, Y.; Wang, L.; Zhan, W. Superior catalytic activity of a Pd catalyst in methane combustion by fine-tuning the phase of ceria-zirconia support. *Appl. Catal. B* **2020**, *266*, 118631–118641.
2. AlMohamadi, H.; Smith, K.J. The impact of CeO_2 Loading on the activity and stability of PdO/γ-AlOOH/γ-Al_2O_3 monolith catalysts for CH_4 oxidation. *Catalysts* **2019**, 9, 557–571
3. Yang, J.; Peng, M.; Ren, G.; Qi, H.; Zhou, X.; Xu, J.; Deng, F.; Chen, Z.; Zhang, J.; Liu, K.; Pan, X.; Liu, W.; Su, Y.; Li, W.; Qiao, B.; Ma, D.; Zhang, T. A hydrothermally stable irreducible oxide-modified Pd/$MgAl_2O_4$ catalyst for methane combustion. *Angew. Chem.* **2020**, 59, 18522–18526
4. Wang, W.; Zhou, W.; Li, W.; Xiong, X.; Wang, Y.; Cheng, K.; Kang, J.; Zhang, Q.; Wang, Y. In-situ confinement of ultrasmall palladium nanoparticles in silicalite-1 for methane combustion with excellent activity and hyrothermal stability. *Appl. Catal. B* **2020**, 276, 119142–119150
5. Chen, Y.; Lin, J.; Chen, X.; Fan, S.; Zheng, Y. Engineering multicomponent metal-oxide units for efficient methane combustion over palladium-based catalysts. *Catal. Sci. Technol.* **2020**, 11, 152–161
6. Petrov, A.W.; Ferri, D.; Kröcher, O.; van Bokhoven, J.A.; Design of stable palladium-based zeolite catalyst for complete methane oxidation by postsynthesis zeolite modification. *ACS Catal.* **2019**, 9, 2303–2312
7. Lim, J.B.; Jo, D.; Hong, S.B. Palladium-exchanged small-pore zeolites with different cage systems as methane combustion catalysts. *Appl. Catal. B* **2017**, 219, 155–162
8. Hosseiniamoli, H.; Setiawan, A.; Adesina, A.A.; Kennedy, E.M.; Stockenhuber, M. The stability of Pd/TS-1 and Pd/silicalite-1 for catalytic oxidation of methane – understanding the role of titanium. *Catal. Sci. Technol.* **2020**, 10, 1193–1204
9. Toso, A.; Colussi, S.; Llorca, J.; Trovarelli, A. The dynamics of PdO-Pd phase transfromation in the presnece of water over Si-doped Pd/CeO_2 methane oxidation catalysts. *Appl Catal. A* **2019**, 574, 79–86
10. Toso, A.; Colussi, S.; Padigapaty, S.; de Leitenburg, C.; Trovarelli, A. High stability and activity of solution combustion synthesized Pd-based catalysts for methane combustion in presence of water. *Appl. Catal. A* **2018**, 230, 237–245
11. Hong, E.; Kim, C.; Lim, D.-H.; Cho, H.-J.; Shin, C.-H. Catalytic methane combustion over Pd/ZrO_2 catalysts: Effect of crystalline structure and textural properties. *Appl. Catal. B* **2018**, 232, 544–552
12. Kim, C.; Hong, E.; Shin, C.-H. Improvement of methane combustion activity for Pd/ZrO_2 catalyst by simple reduction/reoxidation treatment. *Catalysts* **2019**, 9, 838–852